



**HAL**  
open science

## Comparison of Streamflow Estimated by Image Analysis (LSPIV) and by Hydrologic and Hydraulic Modelling on the French Riviera During November 2019 Flood

Sarah Vigoureux, Léa-Linh Liebard, Aubin Chonoski, Etienne Robert, Louis Torchet, Valentin Poveda, Frédérique Leclerc, Jérémy Billant, Rémi Dumasdelage, Gauthier Rousseau, et al.

### ► To cite this version:

Sarah Vigoureux, Léa-Linh Liebard, Aubin Chonoski, Etienne Robert, Louis Torchet, et al.. Comparison of Streamflow Estimated by Image Analysis (LSPIV) and by Hydrologic and Hydraulic Modelling on the French Riviera During November 2019 Flood. *Advances in Hydroinformatics*, Springer Nature Singapore, pp.255-273, 2022, Springer Water, 10.1007/978-981-19-1600-7\_16 . hal-03781334

**HAL Id: hal-03781334**

**<https://hal.science/hal-03781334>**

Submitted on 16 Nov 2022

**HAL** is a multi-disciplinary open access archive for the deposit and dissemination of scientific research documents, whether they are published or not. The documents may come from teaching and research institutions in France or abroad, or from public or private research centers.

L'archive ouverte pluridisciplinaire **HAL**, est destinée au dépôt et à la diffusion de documents scientifiques de niveau recherche, publiés ou non, émanant des établissements d'enseignement et de recherche français ou étrangers, des laboratoires publics ou privés.

## COMPARISON OF STREAMFLOW ESTIMATED BY IMAGE ANALYSIS (LSPIV) AND BY HYDROLOGIC AND HYDRAULIC MODELLING ON THE FRENCH RIVIERA DURING NOVEMBER 2019 FLOOD.

Sarah VIGOUREUX<sup>1</sup>, Léa-Linh LIEBARD<sup>1</sup>, Aubin CHONOSKI<sup>1</sup>, Etienne ROBERT<sup>1</sup>, Louis TORCHET<sup>1</sup>, Valentin POVEDA<sup>1</sup>, Frédérique LECLERC<sup>2</sup>, Jérémy BILLANT<sup>2</sup>, Rémi DUMASDELAGE<sup>3</sup>, Gauthier ROUSSEAU<sup>5</sup>, Olivier DELESTRE<sup>4</sup> & Pierre BRIGODE<sup>2</sup>

<sup>1</sup>Polytech Nice Sophia, Université Côte d'Azur, France

<sup>2</sup>Université Côte d'Azur, CNRS, OCA, IRD, Géoazur, Nice, France

<sup>3</sup>Metropole Nice Côte d'Azur and Nice Municipality, Nice, France

<sup>4</sup>Laboratoire de Mathématiques J.A. Dieudonné, Université Côte d'Azur, Nice, France

<sup>5</sup>Geosciences Rennes, UNR 6118, Université de Rennes, 1, CNRS, Rennes, France

### ABSTRACT

*Short and heavy rainstorm events often lead to flash floods on the French Riviera coastal catchments: during the historical 2nd October 2015 flood, a peak streamflow value between 185 and 295 m<sup>3</sup>/s was estimated on the Brague River at Biot at 10:30 P.M., while the streamflow was around 1 m<sup>3</sup>/s at 6:30 P.M. at the same section. If the measurements of such streamflow values are highly important (for flood statistical analysis, flood modeling, hydraulic structure design), such measurements are dangerous when they require an operator to manipulate an instrument in or near the river. Alternative methods can be used, such as video analysis, by analyzing a sequence of images and locating the displacement of patterns on the water surface. Thus, the velocity field at the flow surface can be determined and then used for estimating flow discharge on specific cross sections. In this work, we applied two different Large-Scale Particle Image Velocimetry (LSPIV) algorithms (Fudaa-LSPIV and OpyFlow) to several videos of the November 2019 floods within the Brague catchment, in order to estimate streamflow values. The obtained streamflow values have then been compared to values estimated through available observations, and also to the results of (i) rainfall-runoff modeling and (ii) hydraulic modeling on the same sections. Both LSPIV estimations, rainfall-runoff simulations and observations are coherent on the studied sections, showing the interest of combining such different and independent techniques in order to estimate flood streamflow values.*

### KEY WORDS

Gauging, LSPIV, hydraulic modelling, hydrologic modelling, 2019 flood.

## 1. INTRODUCTION

Flash floods can be defined as events with a large increase in flow discharges for a short period of time. These events are often observed after rapid and intense rainfall episodes. For example, during the historical flood of October 2, 2015 on the French Riviera, a rainfall accumulation of nearly 300 [mm] was recorded over a 2-h period, with a peak of nearly 100 [mm] in 15 [min]. A peak flow discharge was estimated between 185 and 295 [m<sup>3</sup>/s] at 10:30 PM at the Brague limnometric station in Biot for this episode, whereas the flow rate was approximately 1 [m<sup>3</sup>/s] at 6:30 PM on the same day, at the same location. The rapidity of these episodes makes them difficult to observe. Moreover, the flow discharges during flash floods are often not well known because the observations from limnometric stations are uncertain and the gauging of flood streamflows is very dangerous for an operator. These events are often accompanied by extensive damages to property and the loss of several people. Following the 2015 episode, the Maritime Alps prefecture counted 20 deaths and the damages were estimated to more than 600 Me by the Caisse Centrale de Réassurance [3]. Following the numerous intense meteorological events observed on the French Riviera in recent years and notably in 2019, it seems interesting to study these phenomena in order to better understand them. This is why the modelling and streamflow measurement of flash flood episodes must be improved.

The following work explains how video analysis can be used in parallel with the usual methods for observing flow discharges using limnometric stations. In this study, two Large-Scale Particle Image Velocimetry (LSPIV) algorithms have been used. The first objective of the study is to analyze videos captured on a section of the Brague river and other videos captured on a section of the Valmasque (tributary of the Brague river) during the flood of November 23, 2019. These discharges obtained by image analysis will then be compared with the results of (i) a rainfall-runoff model and (ii) a calculation code for hydraulic modelling on the same basins and sections.

## 2. DATA

In this section, all data used for image analysis (surface and terrain elevation data, bathymetric profile extracted, videos), for rainfall-runoff modelling (terrain for delineation of catchment area and hydrographic network, precipitation) and for hydraulic modelling (terrain elevation, precipitation) are illustrated. Observed flow data are also presented and will be used for validation of the flow discharges estimated by video analysis and by hydrological and hydraulic modelling. All the data used are illustrated on Fig. 1 and will be presented in the following sections.

### 2.1 Studied area

The Brague River is a coastal river located on the French Riviera, near Antibes in the Alpes-Maritimes (Fig. 1 d, e). It is a Mediterranean watershed of 72 [km<sup>2</sup>] at its outlet with several tributaries including the Valmasque. The Brague river catchment is characterised by marked elevations in the upper hills of the basin and an urbanised lower part in the floodplain near the coast. The Brague is regularly confronted with flash floods whose impacts are particularly important due to their unpredictable character. In this study two sub-basins of the Brague will be studied. The Brague at Biot (noted Brague@Biot hereafter) is a sub-catchment of 42 [km<sup>2</sup>], and the Valmasque at Sophia-Antipolis (noted Valmasque@Pipe hereafter) is a sub-catchment of 10 [km<sup>2</sup>], both of which have a hilly landscape with little urbanisation. The two sub-catchments and their associated outlets are illustrated on Fig. 1 d, e

### 2.2 Terrain Elevation and Surface

Two types of elevation data have been used to estimate the streamflows during the November 2019 flood. On one hand, we used a Digital Terrain Model (DTM) from the National Geographic Institute (IGN) at 5 [m] resolution over the whole department [10]. We used this DTM for hydrological and hydraulic modeling at the catchment scale. On the other hand, local Digital Surface Models (DSM) are available on two sections of the Brague and Valmasque rivers obtained by Structure from Motion techniques. Optical images were acquired in

2020, during period of low water, by drones and were processed using a photogrammetry software (3DF Zephyr) to create a terrain elevation model and an orthophotograph (Fig. 1f, g).

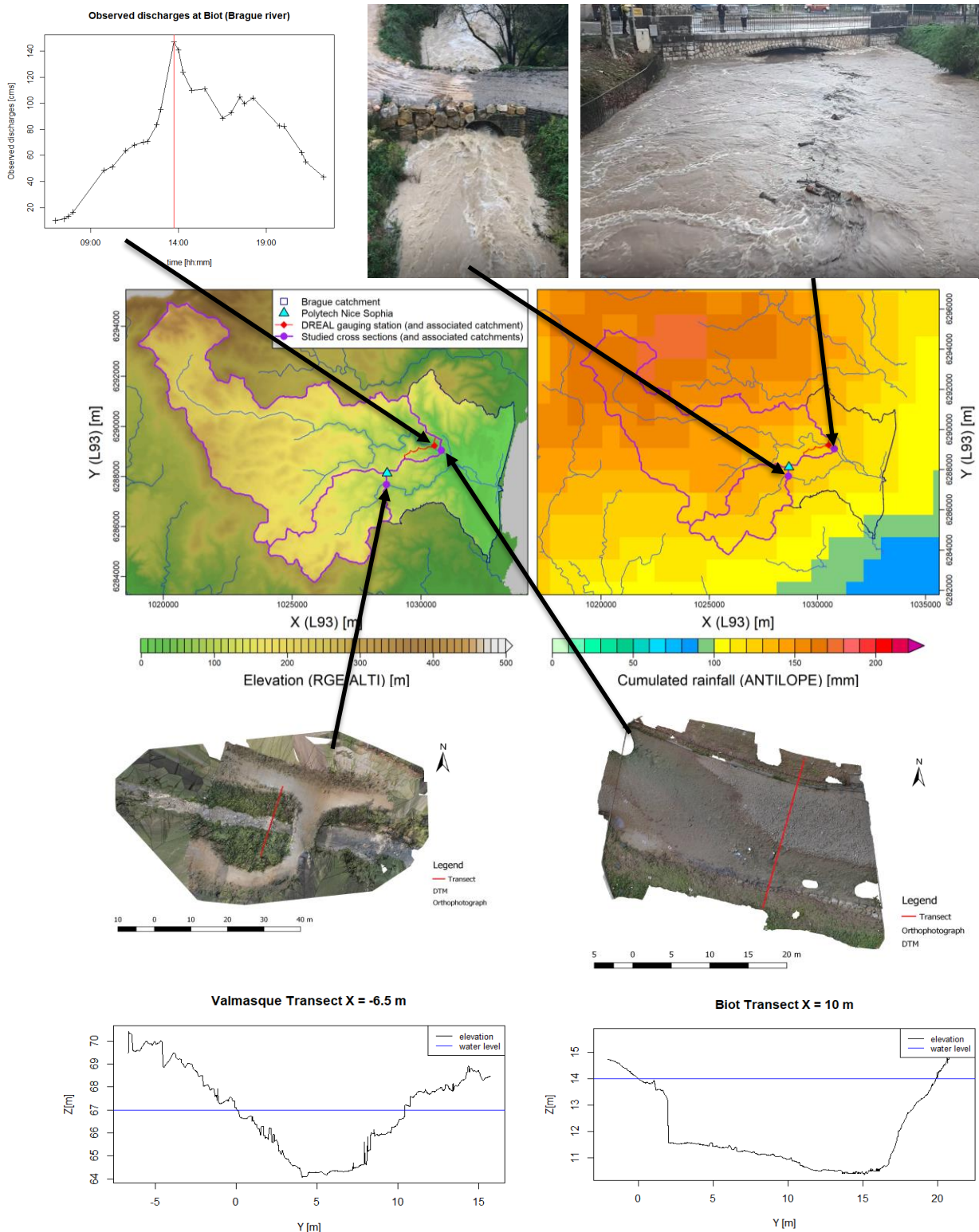


**Figure 1:** 1<sup>st</sup> row: Discharges observed at Biot on the Briage river (left), extract of the video taken on the Valmasque tributary the 23/11/2019 at 13h19 (center), extract of the video taken from the pedestrian bridge of Briage on the Briage river the 23/11/2019 at 13h05 (right). 2<sup>nd</sup> row : IGN DEM (left) and cumulated rainfall from the ANTILOPE database of Meteo-France (right). 3<sup>rd</sup> row : DTM obtained by drone photogrammetry for the Briage river at the Briage pedestrian bridge (top left) and for the Valmasque river (bottom left). 4<sup>th</sup> row: Transects elevation and water level for the Briage river (top right) and for the Valmasque tributary (bottom right).

These models are only available on small portions (where the videos of the 2019 flood have been captured and are of higher resolution (cells of 5 [cm] for the Brague river and 13 [cm] for the Valmasque tributary). They allowed us to extract river cross-sections (bathymetric transects, Fig. 1h, i) that are used to estimate the streamflow with the video analysis software. In addition, the DSMs obtained by drone and the orthophotographs allow us to observe the morphology of the two sites studied. Indeed, we can observe that the banks of the Valmasque are densely vegetated and that the river bottom is made up of fine material up to blocks of about 1 [m] in diameter, whereas the coarser materials at the bottom of the Brague are about 50 [cm] diameter, and the banks are grassed, but the vegetation is less dense. This information will allow us to choose which velocity coefficient to adopt during the image analysis and which roughness coefficient to adopt for the hydraulic modelling.

### 2.3 Rainfall

To carry out the rainfall-runoff and hydraulic modelling, the rainfall data from the “ANTILOPE J + 1” database of Météo France is used. This reanalysis is available 24 h after the event and is built from the rainfall observed with radars corrected with data from Météo-France’s rain gauges [14]. We have a continuous series of rainfall from 2019-11-22 00:00 A.M. to 2019-11-25 00:00 A.M. in 15 [min] time steps, with a resolution of 1 [km<sup>2</sup>] over the entire catchment area. The cumulative rainfall from ANTILOPE data on 23 November 2019 is illustrated on Fig. 1e background, according to these data the rainfall reached 180 [mm] in the Brague catchment and up to 140–150 [mm] in the Valmasque catchment.

### 2.4 Videos

Several video sequences were captured during the flood of 23rd November 2019 on the Brague@Biot and in Sophia-Antipolis on the Valmasque@Pipe. These videos, captured with two different type of cellphones, represent the surface of the water and the material transported at the surface during the flood.

#### *Videos Used for Fudaa-LSPIV*

For the Fudaa-LSPIV software (described in Sect. 16.3.1.1), two video sequences have been used for each section in this study: other videos do not have 10 [s] of stable recording or the angle of the video shot did not allow us to visualise a bank sufficiently, making the orthorectification step of the video analysis difficult. The two videos that will be analysed on the Valmasque@Pipe have been taken on November, the 23rd of 2019 at 1:19 P.M. and 1:20 P.M. and the two videos on the Brague@Biot have been taken on the same day at 1:05 P.M. and 1:29 P.M. Figure 16.1b, c shows an extract from these two videos of the November 2019 floods on the Brague.

#### *Videos Used for OpyFlow*

Two additional videos of the Brague@Biot have been analyzed with the OpyFlow application (described in Sect. 3.1.2), in order to obtain stream wise velocities and deduce discharge on a unique transect: both videos observing the same flow area between two bridges in a short time interval. The first video taken from the downstream bridge has been recorded on November, the 23rd of 2019 at 2:15 P.M. and the second video has been recorded from the upstream bridge, and has been recorded at 2:27 P.M. These videos have a lower quality compared to the video analyzed with Fudaa-LSPIV. These recordings from two sides allow performing a cross verification of the velocities estimated with OpyFlow algorithm.

### 2.5 Observed discharges

The water heights and flow discharges of the Brague river at Biot are available thanks to a hydrometric station operated by the DREAL (<http://www.hydro.eaufrance.fr/>). The hydrograph (Fig. 1a) illustrates the flow discharges observed at the limnometric station of the Brague in Biot (named DREAL gauging station on Fig. 1c, d) during the day of 23 November 2019. The maximum flow discharge is 147 [m<sup>3</sup>/s] observed at 1:45 P.M. on the Brague river at Biot. None hydrometric station was available on the Valmasque tributary during

November 2019. Nevertheless, the peak discharge on the Valmasque river for the 23-11-2019 event has been estimated around 50 [m<sup>3</sup>/s] by a post-flood analysis [4].

### 3. METHOD AND MODELS

The objective of this study is to determine the flow discharges that have passed through two particular sections. We have several video sequences filming the floods on these sections, our first objective is to use video analysis softwares to obtain an estimate of the streamflows. In a second step, we will set up a hydrological modelling chain to go from the catchment precipitations to the streamflows on these two sections, this model will be calibrated on the observations of flow discharges on the Brague@Biot. Setting up the hydrological modelling will allow us to have a continuous streamflow record on the Valmasque, which is an ungauged basin. The flow discharges estimated by image analysis will then be compared with the flow discharges observed at the Brague station in Biot and the streamflows obtained after hydrological modelling. Finally, a last simulation of the streamflows will be set up thanks to a 2D hydraulic model of simulation of the surface flows by injection of rain distributed on the basin. The flow discharges will be extracted from the results of the hydraulic simulation on the same sections and will be compared to the observed flow discharges, estimated by image analysis and by hydrological modelling. The following sections describe the models and methods used for the image analysis, the implementation of the selected hydrological and hydraulic models and the assumptions that were used in this study.

#### 3.1 LSPIV

##### 3.1.1 Fudaa-LSPIV

Fudaa-LSPIV is a software developed by INRAE allowing the processing of flow image sequences in order to calculate surface velocity fields as well as flows through river sections. The method used is that of LSPIV (Large-Scale Particle Image Velocimetry).

First, a video sequence of at least 10 seconds is required. This sequence will be imported into the software and then corrected during the orthorectification stage.

##### *Orthorectification*

Initially the video sequences obtained from various angles are processed using the Fudaa-LSPIV software. During this first stage of orthorectification, a perspective distortion is applied to the images so that the geometry of each image is superimposed on the others. Finally, the orthorectified images allow a top view of the streamflow. To obtain this result, the presence of identifiable reference points on each image is necessary. These points, whose coordinates are known and entered in the software, are the GRPs (Ground Reference Points) represented with red dots on the DSMs obtained by drone photogrammetry (Fig. 1b, c). These points had been chosen because they are visible on all the video images and easily found on the DSMs, the coordinates of these points were recovered from these DSMs. During this phase, the correction of each pixel is given by the calculation of an orthorectification matrix. The result is a system of 11 equations that can be solved by knowing the coordinates of at least 6 GRPs with different altitudes or 4 GRPs at the water level. The calculations are detailed in an example from [8].

##### *Estimation of the surface velocities*

Next comes the PIV (Particle Image Velocimetry) analysis stage. Using the movement of the tracers (natural or added) present in the water, the software calculates the surface velocities at each point of the transect. Once the orthorectification of the images has been carried out, the surface velocities must be found. Fudaa-LSPIV uses a high-precision surface velocity measurement method. This method calculates the flow surface velocity by measuring the particle displacement (serving as a tracer) as a function of time. The same particle is observed on one image at position P, then on a second image at position P' such that P(x, y, t) and P'(x+dx, y+dy, t+dt) with dt the time between the two images being known. Then a speed can be calculated as:

$$u = -\frac{dx}{dt} \quad (1)$$

$$v = -\frac{dy}{dt} \quad (2)$$

According to Jodeau et al [9] the Fudaa-LSPIV algorithm performs the following actions:

- analysis of the tracers visible on the surface;
- calculation of the correlation between a point in image A and image B separated by a lapse of time (dt) second. This time lapse can be parameterized, and the Fudaa-LSPIV software is accurate to the nearest pixel;
- this calculation is repeated on all the nodes of a calculation grid defined by the operator in an iterative way and makes it possible to obtain a 2D surface velocity field.

Filters are applied to the results in order to calculate the temporal average velocity and to obtain the current lines.

### *Estimation on the discharge*

By knowing the surface velocities and bathymetric profile of a section of the streamflow, it is possible to calculate the discharge through that section. Then, the velocity coefficient is set by the operator allowing to switch from the surface velocity profile to the average velocity profile on vertical profiles. Finally, the flow rate can be calculated using the [21] mid-section method at each point of the transect. The velocity coefficient ( $\alpha$ ) depends on the type of river bottom and the type of flow. For a relatively uniform flow, the coefficient typically varies between 0.75 and 0.95, with an average value of 0.85. This depends mainly on the ratio of depth to height of bottom roughness. Dramais et al. [6] give examples of velocity coefficients summarized in the Table 16.1. As we are studying videos of rivers in flood and the water level is pretty high regarding the size of the river bottom material in the case of the two areas studied, we would tend to go for an “usual” velocity coefficient (0.85). However, we must consider that a bridge and a pipe are present just downstream of the two studied sections which could influence the flows and direct us towards a velocity coefficient close to 1. To quantify the impact of the coefficient choice on our streamflow estimation, we decided to perform the video analysis with several velocity coefficients between 0.8 and 1.0 (0.8, 0.85, 0.9 and 1.0)

**Table I:** example of common values for the velocity coefficient.

Default value (uniform flow, average roughness)	0,85
Extremely low value: non-uniform flow, torrents	0,60
Rough flow: low water level, rough bottom, piedmont river	0,80
Usual values	0,84 – 0,88
Smooth flow: high water levels, smooth bottom, concrete channels, large rivers	0,91
Extremely high value: non-uniform flow, influence of a structure	1,20

### **3.1.2 OpyFlow**

Free surface velocities on the Brague@Biot were also estimated by a new open source Python package called OpyFlow, collecting feature displacements in videos. This velocimetry algorithm was developed by Rousseau [22] to estimate free surface velocities in mountain rivers. As Fudaa-LSPIV software, OpyFlow allows performing basic image analysis procedures such as stabilization or bird eye view transformations. The velocimetry technique is however different, and seems more convenient when image qualities are poor for velocimetry, i.e. when having low signal-to-noise ratio or when velocity information on frames is non-uniform. Inspired by past feature tracking approaches [19], the OpyFlow algorithm estimates the local optical flow of good feature to track [23], i.e. features having optimal contrasts to be tracked. Using this alternative tracking procedure may improve both efficiency and accuracy on velocity estimations (see Annexes C & F of [22] for details on the procedures). The entire algorithm is available on the GitHub repository (<https://github.com/groussea/opyflow>).

### **3.2 Rainfall-Runoff model**

For this study, a semi-distributed event-based model was chosen: KLEM (Kinematic Local Excess Model [1]). This model is a coupling between the SCS-CN model for production and a simplified unit hydrograph routing function. This model can be applied to ungauged basins such as the Valmasque. The input data are the rainfall of the basin and the position of the outlet. The assumptions to be set are the subcatchment Curve Number (CN) and the water velocity on the hills and in the river. CN corresponds to a parameter representative of the "hydrogeological behaviour" of the basin and can be calculated for each basin or sub-basin by cross-referencing information on soil type, land use and antecedent soil moisture content. A high CN (CN = 100) means that all the water that precipitates on the basin will run off, which is the case of certain highly urbanized areas with impermeable soil or when the soil is saturated with water or very dry. On the contrary, a low CN (CN = 40) means that a significant part of the water will infiltrate, which is the case in highly vegetated basins and when the soil is not totally saturated. As an output, a streamflow series is generated for the episode studied.

### Model Description

The SCS (Soil Conservation Service) has developed an empirical formula to determine the proportion of rainfall that will participate in the runoff (net rainfall) from the total rainfall on an area. When rain falls on a basin, a volume is first absorbed by the soil ( $I_a$ ). Only once this volume has been intercepted by the soil does a portion of the water begin to run off ( $q$ ) to the surface. This portion of rainfall changes over time. The net rainfall that will runoff is determined from the heavy rain that precipitated thanks to the formulas (3).

$$q = 0 \quad \text{for} \quad P < I_a$$

$$q = \frac{(P - I_a)^2}{(P - I_a + S)} \quad \text{for} \quad P \geq I_a, \quad (3)$$

with  $q$  the runoff in mm,  
 $P$  the rainfall in mm,  
 $I_a$  Initial absorption in mm,  
 $S$  the soil storage in mm.

The soil storage capacity ( $S$ ) is given by formula (4).

$$S = 254 \left( \frac{100}{CN} - 1 \right), \quad (4)$$

with CN the Curve Number.

This storage capacity depends on one parameter: the Curve Number (CN). CN corresponds to a parameter representative of the "hydrogeological behavior" of the basin and can be calculated for each sub-basin by cross-referencing information of soil type, land use and antecedent soil moisture content.

Finally, SCS analyses show that the infiltration parameter can be set as:

$$I_a = 0.2 \times S, \quad (5)$$

Once the portion of rainfall that will contribute to runoff is calculated, it remains to be determined how it will move over the basin and the flows that will be observed. The flow observed at the outlet is translated by the formula (6).

$$Q(t) = \int_A q [t - \tau(x), x] dx, \quad \tau(x) = \frac{L_h(x)}{v_h} + \frac{L_c(x)}{v_c}, \quad (6)$$

with  $Q(t)$  the discharge in cm/s,  
 $\tau(x)$  the transit time in s,  
 $L_h$  the distance travelled on the hill in m,  
 $v_h$  the velocity on the hill in m/s,  
 $L_c$  the distance travelled in the channel in m,  
 $v_c$  the velocity in the channel in m/s.

The proportion of precipitated water that will run off at each mesh of the catchment area is known at every time  $q(t, x)$ . This water will travel, a fortiori, a distance on the hill ( $L_h$ ) at a velocity  $v_h$  and distance in the channel of the river ( $L_c$ ) at a velocity  $v_c$  to the outlet. At each mesh is therefore assigned a transit time ( $\tau(x)$ ) to



the outlet. At the outlet, the quantity of water that will be observed after a certain period is the sum of the volumes of water that have passed through this basin during this duration.

#### *Model Set Up and Parameters Calibration*

Simulations of flow discharges were carried out using the KLEM model with a CN hypothesis ranging from 40 to 100 on the Brague@Biot and on the Valmasque@Pipe catchments (the two outlets are illustrated by purple points on Fig. 1d, e). The simulated flow discharges were compared with the observed flow discharges for the Brague@Biot and the maximum flow discharge estimated by the DDTM for the Valmasque@Pipe.

In the routing function, the hill velocity ( $v_h$ ) is set at 0.5 [m/s] and the channel velocity ( $v_c$ ) is set at 2 [m/s] to the outlet. These assumptions were chosen based on the [1] study and ongoing work on French Riveira catchments (including the Brague catchment) for the 2015 and 2019 floods [2].

The subcatchment contours have been delimited from the DEM thanks to the TauDEM functions (<https://hydrology.usu.edu/taudem/>). The resulting contours are shown on Fig. 1d, e for the two considered outlets. The subcatchment contours are used for averaging rainfall amount on each considered subcatchments.

### **3.3 Hydraulic model**

#### *Model Description*

Basilisk (<http://Basilisk.fr/>) is an open-source calculation code developed by Popinet [20] that allows the modelling of surface flows and finally to observe water heights and flood extents due to a flood event. The model is based on the resolution of the Saint–Venant equations using a well-balanced finite volume method on an adaptive mesh (for more details see [11, 13]). The implementation of an adaptive mesh is interesting for the modelling of surface flows because this principle allows to apply a low mesh resolution on areas of little interest and a higher resolution on areas with more interest. The choice of the mesh level is made by comparing the water height on the mesh with a refinement threshold set by the operator. The use of the adaptive mesh reduces the calculation time compared to the use of a fixed Cartesian mesh more often used to solve the Saint–Venant equations. Kirstetter et al. [12] used the Basilisk calculation code on the Brague basin at its outlet with the rainfall observed during the 2015 flood.

#### *Model Setup*

The input data are the DTM of the area, the net rainfall and a mask that defines the catchment area. The net rainfall is calculated by applying the SCS-CN method on the ANTILOPE gross rainfall raster. For the hydraulic modelling we chose the same model setup than Kirstetter et al. [12]. The Manning's coefficient is uniform over the whole area and equal to 0.05 [–]. The finest refinement level is a 4 [m] cell and the coarsest refinement level is a 66 [m] cell. The refinement threshold is set at 0.2 [m], when this value is exceeded on a cell it must be divided to reach the next higher refinement level in order to improve accuracy. Initially the river is empty, the simulation has not been initialized with a simulation of channel impoundment. The simulation is carried out from Saturday 23 November 2019 at 9:00 AM for 24 [h].

## **4. RESULTS**

### **4.1 Rainfall-Runoff Simulations**

The gross basin rainfall during the November 2019 episode is illustrated in blue on Fig. 2. The rainy episode in November 2019 is spread over a rather long period, with rainfall distributed in two peaks separated by a lull. There are two peaks on the hyetogram, first a first peak on Friday evening and then rain again all day on Saturday with a peak in the middle of the day that is a little more marked for the Valmasque basin. From the net basin rainfall, discharge simulations were carried out using the KLEM model with a CN hypothesis ranging from 40 to 100 on the Brague@Biot, from the Brague to the limnometric station in Biot and to the nozzle on the Valmasque. Finally, a hypothesis of  $CN = 75$  the simulated flow discharges to be as close as possible to the flow discharges observed at the station on the Brague in Biot. Discharges simulated with the  $CN = 75$  hypothesis is shown in blue line on Fig. 2. The same hypothesis has been retained for the Brague catchment and for the Valmasque tributary even if the peak flow discharge is higher than the 50 [m<sup>3</sup>/s] estimated by the DDTM.

## 4.2 Hydraulic Simulations

On the flow discharge curves extracted from the results of the hydraulic simulations with Basilisk at the sections of the Brague@Biot and the Valmasque@Pipe illustrated in purple on Fig. 3, the flow discharges are equal to zero for a few hours after the beginning of the simulation before increasing, whereas the rain is injected over the whole domain from the beginning of the simulation. This seems to be related to the refinement levels (cell sizes ranging from 66 to a 4 [m]) and refinement threshold (here set at 0.2 [m]) considered. Then, a rather gentle increase in streamflow is observed on the Valmasque followed by a peak flow discharge of about 20 [m<sup>3</sup>/s] on Saturday at 1:00 PM which is far below the DDTM post-flood estimates, the streamflow then starts a very slow decrease to return to the base flow in more than 10 [h]. The chronicle of simulated streamflows on the Brague shows a very sudden increase in flow discharge in a staircase and then a levelling off, a new slower increase in flow discharges reaches a peak of about 100 [m<sup>3</sup>/s] on Saturday at 4:00 P.M. which is followed by a recession that follows the same trend as the observed flow discharges, whereas the peak flow discharge observed on the Brague reaches 147 [m<sup>3</sup>/s] on Saturday at 1:45 P.M. in Biot.

## 4.3 LSPIV Streamflow Estimations

The LSPIV analysis of the videos of the Brague@Biot allows to estimate the flow discharge at  $94 \pm 10$  [m<sup>3</sup>/s] the Saturday (23-11-2019) at 01:05 P.M. and  $140 \pm 15$  [m<sup>3</sup>/s] the Saturday at 01:29 P.M. On the Valmasque@Pipe the videos analysis gives a flow discharge at  $39.1 \pm 4$  [m<sup>3</sup>/s] the Saturday at 01:19 P.M. and  $33 \pm 4$  [m<sup>3</sup>/s] the Saturday at 01:20 P.M. These estimates were made using a velocity coefficient of 0.9 and the confidence interval corresponds to the flows estimated with a velocity coefficient of  $\alpha = 0.9 \pm 0.1$ . The estimated discharges are illustrated in orange on Fig. 3. Then, OpyFlow has been used on two additional videos on the Brague@Biot catchment. Figure 16.4a, b shows 3D visualizations of the velocities collected from the two considered videos, and Fig. 4c shows the projection of the feature tracking point cloud. The flow rate has been estimated at  $101.7 \pm 20$  m<sup>3</sup>/s). As for Fudaa-LSPIV, the uncertainties were estimated using a velocity coefficient  $\alpha = 0.9 \pm 0.1$ , which is in agreement with large submergence flows (see [24] and an uncertainty on the surface position equal to  $\Delta h = 0.2$  [m]. Observed discharge during this time interval is about 120 m<sup>3</sup>/s according to field station estimation.

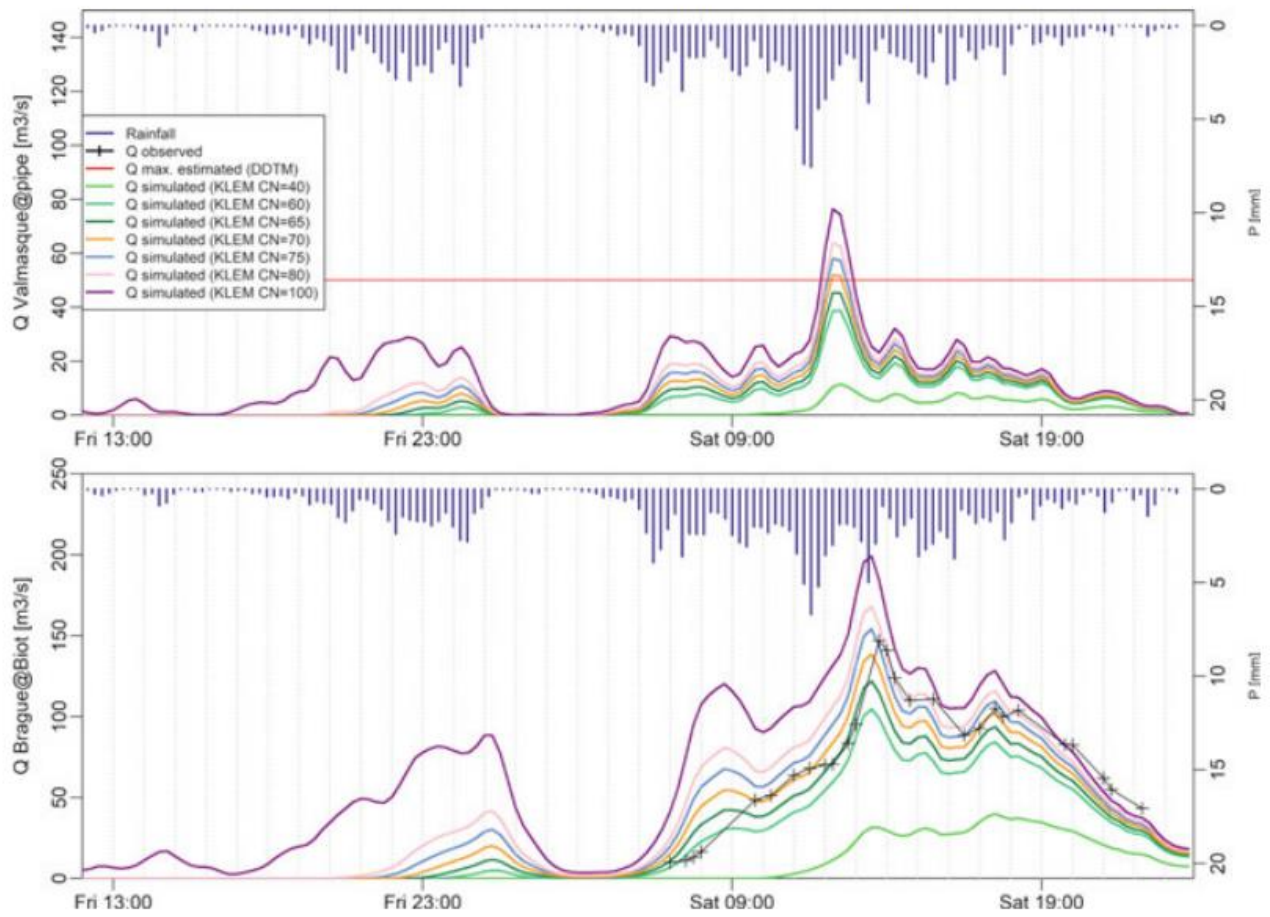


**Fig. 2** Discharges simulated using the KLEM model using a CN = 40, 60, 65, 70, 75, 80 and 100

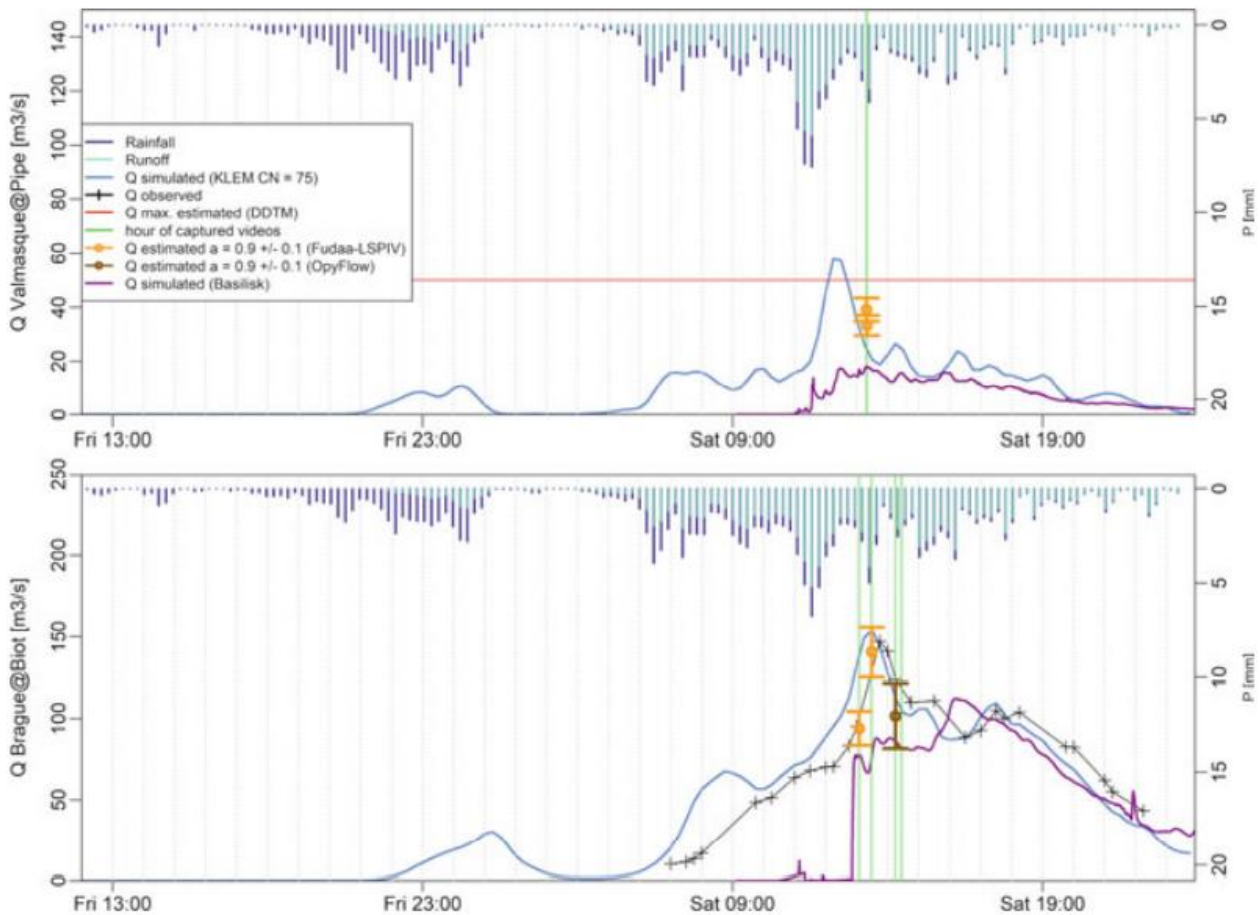


**Fig. 3** Results of the discharges simulations and estimations

#### 4.4 Comparison Between the Streamflow Estimations

On Fig. 3, the gross rainfall and net rainfall obtained by the SCS-CN with an hypothesis of  $CN = 75$  method are illustrated on the higher part of Fig. 3. The flow discharges simulated from the KLEM model application with a hypothesis of  $CN = 75$  for the SCS-CN production function are illustrated in a continuous blue line on the lower part of Fig. 3 and the flow discharges observed at the station on the Brague at Biot are illustrated with a black line crossed by black crosses. On the Valmasque graphic, the red line indicates the maximum flow discharge estimated by the DDTM 06. The light green vertical lines indicate the dates and times when the videos were taken. The orange and brown vertical intervals give the discharges estimations obtained by video analysis, using Fudaa-LSPIV and PoyFlow, respectively. For Fudaa-LSPIV, the circle represents the value of the discharge estimation made with a velocity coefficient of 0.9, the upper boundary is the value of the discharge estimation made with a velocity coefficient of 1.2 and the lower boundary is the value of the discharge estimation made with a velocity coefficient of 0.6. For OpyFlow, the circle represents the value of the discharge estimation made with a velocity coefficient of 0.85. Finally, the flow discharges simulated by hydraulic modelling with Basilisk are shown in purple. On the Brague@Biot catchment, the discharges simulated by rainfall-runoff modelling represent the observations rather well: the trend of the simulated streamflows is rather consistent with the trend of the observed streamflows in terms of dynamics as well as the magnitude, the flood peak is shifted by only a few minutes and the simulated maximum flow discharge value (154 [m<sup>3</sup>/s]) is a little above the observed peak (147 [m<sup>3</sup>/s]). The flow discharge estimates by video analysis are very satisfactory since we can see that the observed flows on the Brague@Biot (in black) 270 S. Vigoureux et al. intersect the vertical bars in orange representing the estimated flow values and we notice that it is the estimated flow discharge value with a velocity coefficient of 0.85 which gives the best estimate. As described above, the flow record from the results of Basilisk simulations on the Brague@Biot is not very consistent with the observations. Indeed, we observe that the flow discharges are equal to zero for about 2 [h] before increasing abruptly. The rise of the simulated hydrograph arrives with a lag of nearly 4 [h] with the

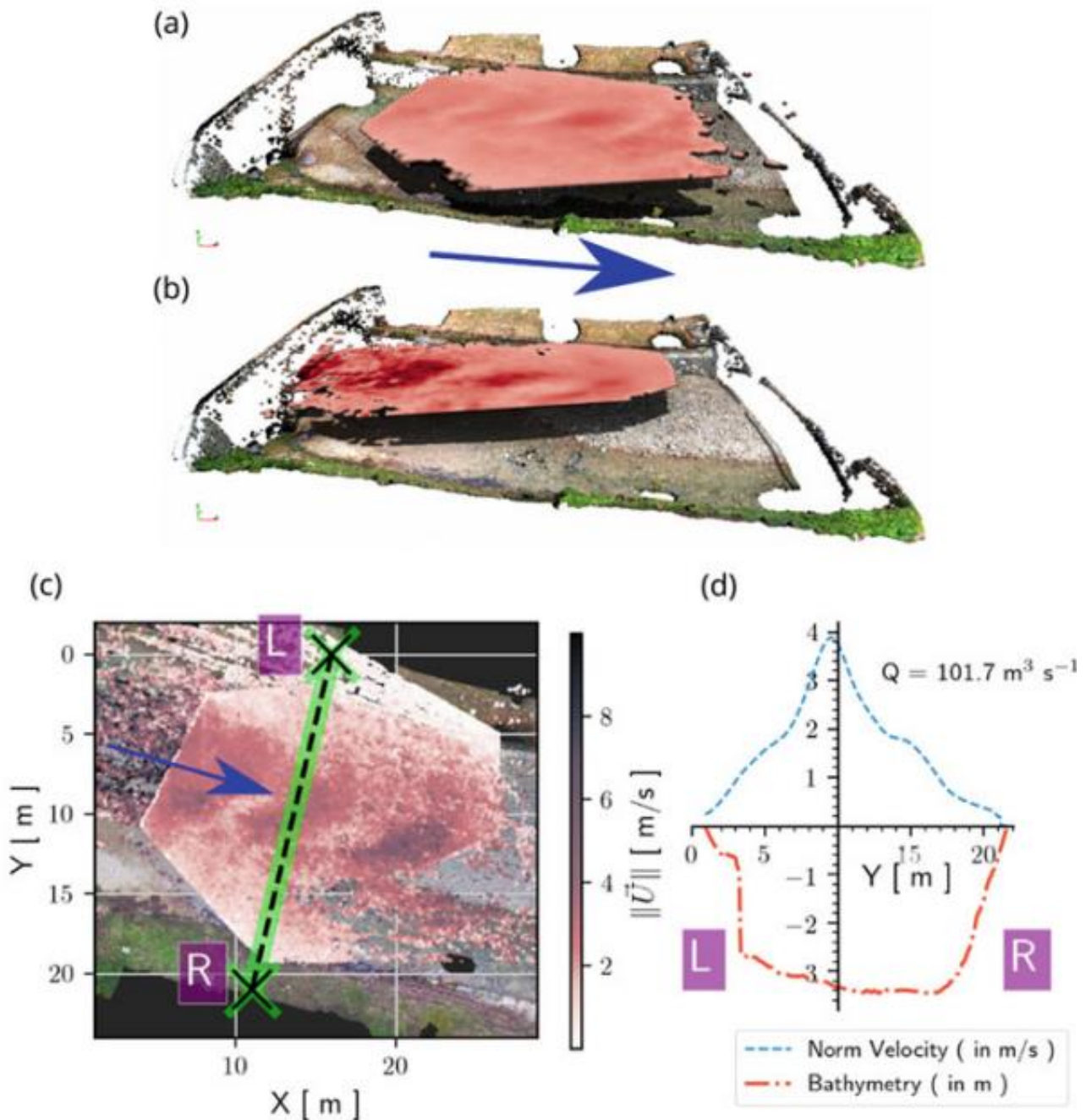


**Fig. 4** Cross verification of free surface velocity estimations performed with OpyFlow on the Brague@Biot. a Free surface velocity estimated with a video captured from the upstream bridge, and b from the downstream bridge. Vertical position of the velocity surfaces are located at the estimated free surface. c Feature tracking velocimetry cloud extracted from the two videos. d Free surface velocity and bathymetry along Y. The flow rate is estimated at  $101.7 \pm 20 \text{ m}^3/\text{s}$

observed rise, the peak of simulated flow discharge is also delayed by nearly 3 [h] and below the observed peak flow discharge. The results on the Valmasque@Pipe catchment are a little less satisfactory, the chronicle of streamflows simulated by rainfall-runoff modelling gives a peak flow discharge above the DDTM estimate, the trend cannot be analysed since we do not have a chronicle of water level or observed flow on this section. The simulated flow discharges overlap with the flow discharge intervals estimated by video analysis but the velocity coefficient that seems to work best seems to be close to 60–70. The two videos available on the Valmasque were taken at almost the same time and the video estimations were carried out in the same way and using the same method (same GRPs, same transect): only the videos change, however it can be observed that the video estimations do not give the same results. The trend in the streamflow chronicle resulting from the Basilisk simulations on the Valmasque is not consistent with the streamflow chronicle obtained by hydrological

modelling. Indeed, we observe that the flows are equal to zero for about 2 [h] before increasing slowly to reach a peak flow discharge of about 20 [m<sup>3</sup>/s] against a little more than 50 [m<sup>3</sup>/s] for the hydrological simulation, a plateau is observed for about 3 [h] then a slow decrease starts following this time very well the trend of the streamflow simulated with the rainfall-runoff model. The flow discharges estimated at 1:19 P.M. and 1:20 P.M. are well above the maximum flow discharges simulated by the hydraulic model, respectively the flow discharges estimated by video analysis are between 22 and 52 [m<sup>3</sup>/s] against a maximum of 20 [m<sup>3</sup>/s] for the hydraulic simulation.

## 5. DISCUSSION

Regarding the flow discharges estimations made by LSPIV analysis, we used the bathymetry of cross-sections extracted from DSM obtained by drone photogrammetry, but by definition the DSM gives the elevation of the surface with the vegetation and not the terrain. On our transects, we considered the surface above the vegetation, but as we can see on the orthophotography and on the videos, the vegetation is rather dense on the banks of the Valmasque and there can be flows which take place in this zone of vegetation on the banks. By not taking into account these flows and by taking the surface of the vegetation as the bottom of the transect we may underestimate the flow through the section. Moreover, there are few tracers on the videos of flows on the Valmasque, which makes the estimate more uncertain than on the Brague, where numerous tracers are visible during the video. The lack of tracers may explain why the two videos gave different results of discharges estimations although they were taken at almost the same time (1 [min] difference) on the same section at the same position and the analysis were made on the same cross-section and using the same GRPs. In addition the better velocity coefficients in our case are close to 0.85 which are common values although we could have thought that the velocity coefficients would take higher values close to 1.2 which corresponds to flows influenced by a hydraulic structure because in the case of our two sections there is a bridge and a pipe downstream. The rainfall-runoff simulation obtained on the Brague@Biot with the KLEM model is the closest to the observed streamflow series when using an  $CN = 70$ . We thus chose to apply the same  $CN$  hypothesis for both basins (Brague@Biot and Valmasque@Pipe) because the soil occupations are more or less similar as well as the soil moisture before the rain event, but we did not study precisely the soil types and the soil occupations of both basins. According to the sensitivity study of the streamflows simulated with respect to the  $CN$  parameter, it seems that a lower  $CN$  (60–70) would correspond better to the Valmasque@Pipe basin, as we can see on Fig. 2. Excessive flow discharges may also be due to an over-estimation of rainfall on the cells of the ANTILOPE database over the Valmasque basin. Finally, the hydraulic simulation performed using Basilisk could be significantly improved by considering different refinement options, and by simulating the entire rainfall event, on the two considered days.

## 6. CONCLUSION

In this study, we applied two different LSPIV techniques on several videos acquired during the 23 November 2019 flood on the Brague catchment in order to estimate the associated streamflow. Obtained results are coherent with available observations, and also with rainfall-runoff simulations performed on the associated catchments. Such comparison are needed in order to better estimate high streamflow values, then used for flood statistical analysis, flood modeling, or hydraulic structure design, and also to use LSPIV techniques on ungauged French Riviera catchments.

**Acknowledgements.** The authors thank Météo-France for providing the meteorological data, IGN for the elevation data and 3DF Zephyr for providing us educational licences that allowed calculating the local high-resolution DTMs used in this study.

## REFERENCES

1. Borga M, Boscolo P, Zanon F, Sangati M (2007) Hydrometeorological analysis of the 29 August 2003 flash flood in the Eastern Italian Alps. *J Hydrometeorol* 8(5):1049–1067. <https://doi.org/10.1175/JHM593.1> 272 S. Vigoureux et al.
2. Brigode P, Vigoureux S, Delestre O, Nicolle P, Payrastre O, Dreyfus R, Nomis S, Salvan L, Inondation sur la Côte d’Azur : bilan hydro-météorologique des épisodes de 2015 et 2019. To be submitted à La Houille Blanche
3. CCR (2016) Les Catastrophes Naturelles en France - Bilan 1982–2016: chiffres clés. Rapport, 60 p
4. DDTM des Alpes-Maritimes - SDRS/Mission RDI Préfecture des Alpes-Maritimes - SIDPC (2020) Retour d’expérience des intempéries des 22–24 novembre et 1–2 décembre 2019 dans les Alpes-Maritimes. Rapport, 155 p
5. Dramais G, Le Coz J, Camenen B, Hauet A (2011) Advantages of a mobile LSPIV method for measuring flood discharges and improving stage-discharge curves. *J Hydro-Environ Res* 5:301–312. <https://doi.org/10.1016/j.jher.2010.12.005>
6. Dramais G, Le Coz J, Le Boursicaud R, Hauet A, Lagouy M (2014) Jaugeage par radar mobile, protocole et résultats. *La Houille Blanche*, 23–29. <https://doi.org/10.1051/lhb/2014025>
7. Hauet A (2016) Monitoring river flood using fixed image-based stations: experience feedback from 3 rivers in France. In: *RiverFlow 2016*, St. Louis, USA, 11–14 July 2016, pp 541–547
8. Jodeau M, Hauet A, Paquier A, Le Coz J, Dramais G (2008) Application and evaluation of LS-PIV technique for the monitoring of river surface velocities in high flow conditions. *Flow Meas Instrum* 19:117–127
9. Jodeau M, Hauet A, Le Coz J, Bodart G (2019) Fudaa-LSPIV version 1.7.3 - Fudaa-LSPIV - La forge logicielle d’Irstea. <https://forge.irstea.fr/news/57>
10. IGN (2018) RGE ALTI version 2.0. Descriptif de contenu, 38 p
11. Kirstetter G, Hu J, Delestre O, Darboux F, Lagrée P-Y, Popinet S, Fullana JM, Josserand C (2016) Modeling rain-driven overland flow: empirical versus analytical friction terms in the shallow water approximation. *J Hydrol* 536:1–9. <https://doi.org/10.1016/j.jhydrol.2016.02.022>
12. Kirstetter G, Bourgin F, Brigode P, Delestre O (2020) Real-time inundation mapping with a 2D hydraulic modelling tool based on adaptive grid refinement: the case of the October 2015 French Riviera Flood. In: *Advances in hydroinformatics*. Springer Water, pp 335–346. [https://doi.org/10.1007/978-981-15-5436-0\\_25](https://doi.org/10.1007/978-981-15-5436-0_25)
13. Kirstetter G, Delestre O, Lagrée P-Y, Popinet S, Josserand C (2021, in review) B-Flood 1.0: an open-source Saint-Venant model for flash flood simulation using adaptive refinement. *Geosci Model Dev Discussions*, 1–24. <https://doi.org/10.5194/gmd-2021-15>
14. Laurantin O (2008) ANTILOPE: hourly rainfall analysis merging radar and rain gauge data. In: *Proceedings of the international symposium on weather radar and hydrology*, Grenoble, France, pp 2–8
15. Le Boursicaud R, Pénard L, Hauet A, Le Coz J (2016) Gauging extreme floods on YouTube: application of LSPIV to home movies for the post-event determination of stream discharges. *Hydrol Process* 30:90–105. <https://doi.org/10.1002/hyp.10532>
16. Le Coz J, Hauet A, Pierrefeu G, Dramais G, Camenen B (2010) Performance of image-based velocimetry (LSPIV) applied to flash-flood discharge measurements in Mediterranean rivers. *J Hydrol* 394(1–2):42–52. <https://doi.org/10.1016/j.jhydrol.2010.05.049>

17. Le Coz J, Jodeau M, Hauet A, Marchand B, Le Boursicaud R (2014) Image-based velocity and discharge measurements in field and laboratory river engineering studies using the free FUDAA-LSPIV software. In: River Flow 2014, Lausanne, Switzerland, 7 p
18. Le Coz J, Patalano A, Collins D, Federico Guillén N, García CM, Smart GM, Bind J et al (2016) Crowdsourced data for flood hydrology: feedback from recent citizen science projects in Argentina, France and New Zealand. *J Hydrol* 541:766–777. <https://doi.org/10.1016/j.jhydrol.2016.07.036>
19. Miozzi M, Jacob B, Olivieri A (2008) Performances of feature tracking in turbulent boundary layer investigation. *Exp Fluids* 45(4):765. <https://doi.org/10.1007/s00348-008-0531-3>
20. Popinet S (2011) Quadtree-adaptive tsunami modelling. *Ocean Dyn* 61(9):1261–1285. <https://doi.org/10.1007/s10236-011-0438-z>
21. Rantz SE et al (1982) Measurement and computation of streamflow: Volume 1. Measurement of stage and discharge. USGS. 2175
22. Rousseau G (2019) Turbulent flows over rough permeable beds in mountain rivers: experimental insights and modeling. Thèse de doctorat, EPFL. <https://doi.org/10.5075/epfl-thesis-9327>
23. Shi J (1994) Good features to track. In: IEEE conference on vision and pattern recognition. IEEE
24. Welber M, Le Coz J, Laronne JB, Zolezzi G, Zamler D, Dramais G, Hauet A, Salvaro M (2016) Field assessment of noncontact stream gauging using portable surface velocity radars (SVR). *Water Resour Res* 52:1108–1126. <https://doi.org/10.1002/2015WR017906>